Suplemento de la Revista Mexicana de Física **3** 0308068 (2022) 1–5

Quantum computation of heavy quarkonium masses

D. Gallimore and J. Liao

Department of Physics, Indiana University Bloomington, Bloomington, United States.

Received 24 December 2021; accepted 20 April 2022

We perform a quantum calculation of the 1S charmonium mass by simulating the spinless Cornell Hamiltonian on a quantum processor using a variational method. Errors due to a global depolarizing noise channel are corrected with a zero-noise extrapolation method, resulting in good agreement with the known value. We also calculate the 2S mass of charmonium on a noiseless quantum simulator by orthogonalizing with respect to the ground state. This research demonstrates that near-term quantum devices are capable of simulating heavy quark bound states, which are currently under-represented in the literature.

Keywords: Quantum computing; variational quantum eigensolver; Cornell potential; quark bound state; error mitigation.

DOI: https://doi.org/10.31349/SuplRevMexFis.3.0308068

1. Introduction

In recent years, the intersection between quantum computing and nuclear physics has experienced major developments at a rapid pace [1–3]. While a full simulation of QCD is not yet practical, quantum computers are currently capable of simulating effective models of the strong force as well as related gauge field theories (*e.g.*, in lower dimensions and/or with smaller symmetry groups) [4–17]. Recently, quantum computations of the ground state energies of few nucleon systems have been achieved using variational quantum eigensolver (VQE) methods [4, 5], extending the usefulness of quantum algorithms into the subatomic realm. However, simulations of systems of quarks/antiquarks remain under-represented in the literature. In this document, we present a quantum computation of the ground state mass of charmonium, a bound state between charm and anticharm quarks, using a spin-averaged potential. We choose to study charmonium since interactions between heavy quarks are approximately nonrelativistic, simplifying their dynamics. Our calculation uses the VQE algorithm [18] with unitary coupled cluster (UCC) ansatz [18, 19]. To correct errors due to decoherence, we employ a zero-noise extrapolation method. We also describe a method for calculating masses of excited charmonium states, and implement it on a noiseless quantum simulator to calculate the mass of the first excited state. Further details of this study can be found in [20].

2. The Hamiltonian

Up to spin corrections, heavy quark-antiquark bound states are described by the effective potential

$$V(r) = -\frac{\kappa}{r} + \sigma r, \tag{1}$$

known as the Cornell potential [21]. We set $\kappa = 0.4063$ and $\sqrt{\sigma} = 441.6$ MeV. The Cornell potential enters into the Hamiltonian

$$H_N = \sum_{m,n=0}^{N-1} \langle m| (T+V) |n\rangle \, a_m^\dagger a_n, \tag{2}$$

which is truncated after N orbitals. In our simulations, we set $N = 3$ to save on computational resources. The operators $a_n^\dagger$ and a_n create and annihilate a c-$\bar{c}$ pair in the harmonic oscillator s-wave state $|n\rangle$. We choose the frequency of the harmonic oscillator to be $\omega = 562.9$ MeV, which corresponds to a length scale of about 0.35 fm. This is similar in size to known charmonium states.

To be useful in a quantum calculation, the Hamiltonian must be written in terms of quantum gates and the state of the c-$\bar{c}$ pair must be mapped to a collection of qubits. To accomplish the former, we employ the Jordan-Wigner transformation,

$$a_n^\dagger = \frac{1}{2}\left(\prod_{j=0}^{n-1} Z_j\right)(X_n - iY_n), \tag{3}$$

$$a_n = \frac{1}{2}\left(\prod_{j=0}^{n-1} Z_j\right)(X_n + iY_n), \tag{4}$$

which uses the abbreviated notation $X_n \equiv \sigma_n^x$, $Y_n \equiv \sigma_n^y$, and $Z_n \equiv \sigma_n^z$ for Pauli operators acting on the nth qubit. The state of the system is of the form $|f_N \cdots f_2 f_1\rangle$, where each f_n represents the number of c-$\bar{c}$ pairs in the nth harmonic oscillator s-wave state. Since there exists at most one pair in any given harmonic oscillator state, each f_n can straightforwardly be identified with a qubit. The Hamiltonian $H_3 = \sum_{i=0}^{9} H_3^i$ used in this research is a sum of 10 terms:

$$H_3^0 = \frac{1}{2}\left(\frac{21}{4}\omega + V_{00} + V_{11} + V_{22}\right), \tag{5}$$

$$H_3^1 = -\frac{1}{2}\left(\frac{3}{4}\omega + V_{00}\right) Z_0, \tag{6}$$

$$H_3^2 = -\frac{1}{2}\left(\frac{7}{4}\omega + V_{11}\right) Z_1, \tag{7}$$

$$H_3^3 = -\frac{1}{2}\left(\frac{11}{4}\omega + V_{22}\right) Z_2, \tag{8}$$

$$H_3^4 = \frac{1}{4}\left(-\sqrt{\frac{3}{2}}\omega + 2V_{01}\right) X_0 X_1, \tag{9}$$

$$H_3^5 = \frac{1}{4}\left(-\sqrt{5}\omega + 2V_{12}\right) X_1 X_2, \tag{10}$$

$$H_3^6 = \frac{1}{4}\left(-\sqrt{\frac{3}{2}}\omega + 2V_{01}\right) Y_0 Y_1, \tag{11}$$

$$H_3^7 = \frac{1}{4}\left(-\sqrt{5}\omega + 2V_{12}\right) Y_1 Y_2, \tag{12}$$

$$H_3^8 = \frac{1}{2} V_{02} X_0 Z_1 X_2, \tag{13}$$

$$H_3^9 = \frac{1}{2} V_{02} Y_0 Z_1 Y_2, \tag{14}$$

with $V_{mn} \equiv \langle m| V |n\rangle$. One of the terms is proportional to the identity, while the other nine are proportional to traceless unitary operators.

3. Application of VQE

The variational principle states that, given an ansatz $|\psi(\vec{\theta})\rangle$ and the Hamiltonian H_3,

$$\langle\psi(\vec{\theta})| H_3 |\psi(\vec{\theta})\rangle \geq \epsilon_0, \tag{15}$$

where ϵ_0 is the ground state energy of H_3. This principle forms the basis of the VQE algorithm, which uses a classical optimization procedure to minimize $\langle H_3\rangle$ with respect to the parameters $\vec{\theta}$ and a quantum subroutine to calculate $\langle H_3\rangle$ for any given $\vec{\theta}$. Although the VQE algorithm is primarily used to estimate ϵ_0, it can be improved to systematically estimate excited state energies as well. Let $|\psi(\vec{\theta}_0)\rangle$ be the ground state wave function and let $|\psi(\vec{\theta}_1)\rangle$ satisfy

$$\langle\psi(\vec{\theta}_1)| H_3 |\psi(\vec{\theta}_1)\rangle = \epsilon_1, \tag{16}$$

where $\epsilon_1 > \epsilon_0$ is the energy of the first excited state. One can show that for all states $|\psi(\vec{\theta})\rangle$ orthogonal to the ground state,

$$\langle\psi(\vec{\theta})| H_3 |\psi(\vec{\theta})\rangle \geq \epsilon_1 > \epsilon_0. \tag{17}$$

In other words, if the ansatz is orthogonalized with respect to the ground state wave function, the variational method gives an upper bound on the next lowest eigenvalue. This is true even if the ground state is approximate. One can apply this technique iteratively to estimate any excited state energy. In practice, however, the largest excited state that one can estimate is limited by the number of truncated basis orbits in an actual calculation. In a more general context, we note this strategy is essentially an application of the so-called Hylleraas-Undheim-MacDonald theorem [22, 23].

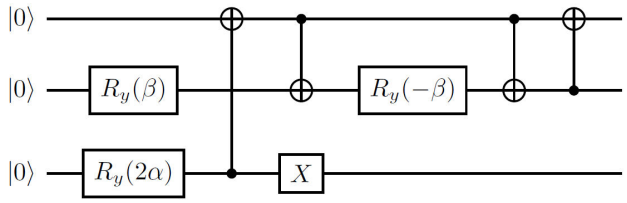

FIGURE 1. A low-depth gate decomposition of the ansatz used in our simulations.

We approximate the ground state energy of H_3 using the VQE algorithm in tandem with the UCC ansatz. For a single c-$\bar{c}$ pair with access to three orbitals, this ansatz consists only of the unitary operator

$$U(\theta,\phi) = \exp\left\{\theta(a_1^\dagger a_0 - a_0^\dagger a_1) + \phi(a_2^\dagger a_0 - a_0^\dagger a_2)\right\}, \tag{18}$$

which rotates the state $|001\rangle$ into a linear combination of $|001\rangle$, $|010\rangle$, and $|100\rangle$ with coefficients tuned by θ and ϕ. For this specific system, however, it is more convenient to use the parameters α and β, defined by $\alpha \equiv \sqrt{\theta^2+\phi^2}$ and $\sin\beta \equiv \theta/\alpha$. The 3-qubit UCC ansatz for a single c-$\bar{c}$ pair is then just

$$|\psi(\alpha,\beta)\rangle = \cos\alpha\,|001\rangle + \sin\alpha\sin\beta\,|010\rangle + \sin\alpha\cos\beta\,|100\rangle\,. \tag{19}$$

A low-depth gate decomposition of $|\psi(\alpha,\beta)\rangle$ is illustrated in Fig. 1. After approximating the ground state using VQE, we approximate the first excited state by employing the corollary discussed in the previous paragraph.

4. Error mitigation

4.1. Noise scaling

To compute $\langle H_3\rangle$ on a quantum computer with respect to the variational ansatz, we must measure each of the 9 traceless unitary operators that appear in the Hamiltonian separately. On a real quantum computer, each of these measurements will be influenced by amplitude damping, phase damping, or depolarizing noise channels [24]. Of these, we choose to correct for a potential depolarizing channel. Though this channel usually overestimates the degree to which quantum information is lost to the environment, it is appropriate since we have no detailed information about the actual physical noise channel of the quantum computer we are using.

To correct for a potential global depolarizing channel, we employ a zero-noise extrapolation method based on [25]. Let

$$U = L_d \cdots L_2 L_1 \tag{20}$$

be an N-qubit quantum circuit with depth d. Each layer L_i is composed of one or more quantum gates that can be executed simultaneously. Assuming a global depolarizing channel is

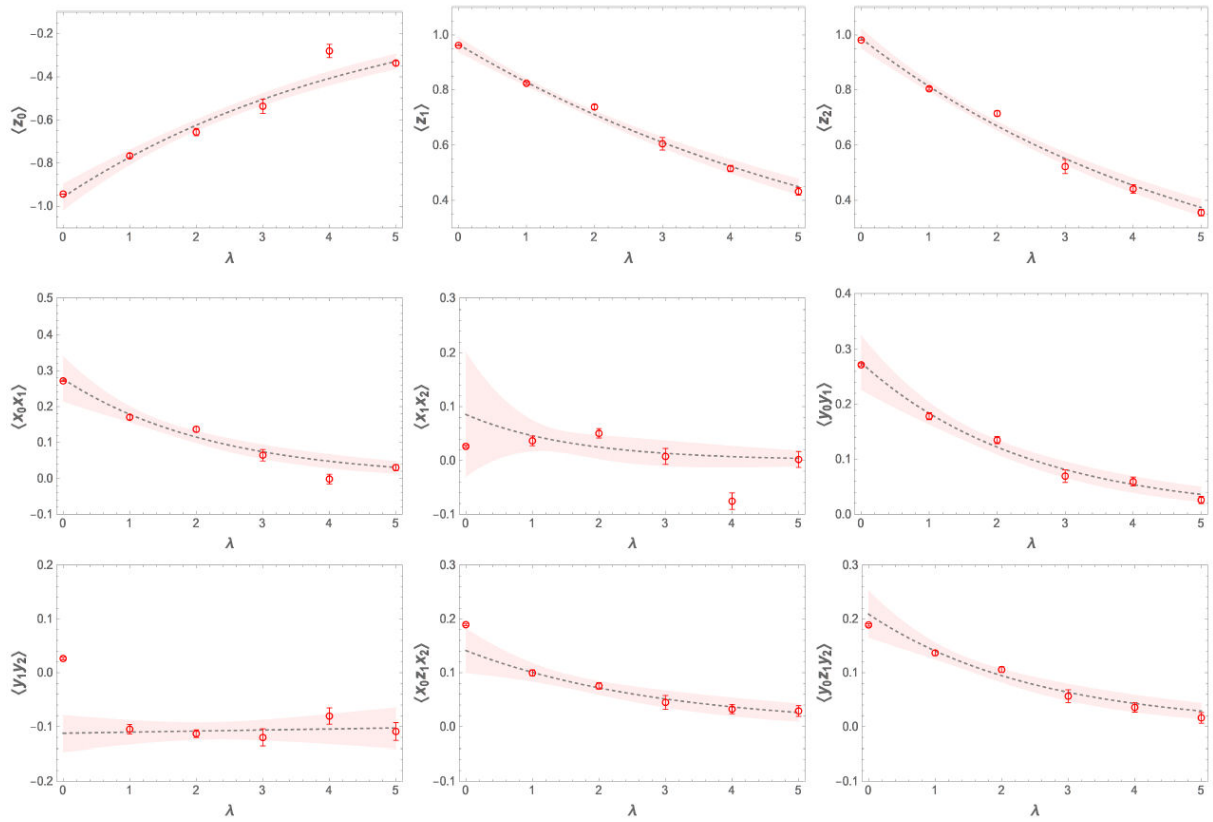

FIGURE 2. Expectation values (in Mev) of each H_3^i versus the scaling parameter λ with 95% confidence mean prediction bands. Noiseless quantum simulation results are indicated by stars, but are not included in the fits.

the dominant source of noise in the circuit, ρ transforms under L_i in a way that depends only on an ideal noiseless part $\tilde{L}_i$ and a layer-dependent success rate $0 \leq r_i \leq 1$. That is,

$$\rho \xrightarrow{L_i} r_i \tilde{L}_i \rho \tilde{L}_i^\dagger + \frac{1}{2^N}(1 - r_i) I. \tag{21}$$

Consequently, ρ transforms like

$$\rho \xrightarrow{U} r \tilde{U} \rho \tilde{U}^\dagger + \frac{1}{2^N}(1 - r) I \tag{22}$$

under the circuit U, with total success rate $r \equiv \prod_{i=1}^{d} r_i$.

While U will have a base level of noise that cannot be controlled, it is possible to scale the presence of noise in a predictable manner. Consider the new circuit

$$V \equiv U(U^\dagger U)^n (L_1^\dagger \cdots L_s^\dagger)(L_s \cdots L_1), \quad 0 \leq s < d. \tag{23}$$

While V is logically equivalent to U, the ratio of their depths is

$$\kappa \equiv 2\frac{s}{d} + 2n + 1. \tag{24}$$

Under this larger circuit, ρ transforms like

$$\rho \xrightarrow{V} r^\lambda \tilde{U} \rho \tilde{U}^\dagger + \frac{1}{2^N}(1 - r^\lambda) I, \tag{25}$$

where

$$\lambda \equiv 2\frac{\ln q}{\ln r} + 2n + 1 \tag{26}$$

is a noise scaling parameter and $q \equiv \prod_{i \leq s} r_i$. In the simplest case where $s = 0$, the additional noise introduced by V depends only on circuit depth since $\lambda = \kappa$. This is the scaling behavior given the most attention in [25]. However, in the general case where $0 \leq s < d$, knowledge of the depths alone is not sufficient.

4.2. Zero-noise Extrapolation

The expectation value of a traceless unitary operator A with respect to V is

$$\langle A \rangle (\lambda) = \langle \tilde{0} | \tilde{U}^\dagger A \tilde{U} | \tilde{0} \rangle r^\lambda. \tag{27}$$

Evidently, $\langle A \rangle (\lambda)$ is proportional to the noiseless expectation value, but vanishes exponentially quickly as λ increases beyond 1. One estimates the noiseless result by measuring $\langle A \rangle (\lambda)$ for various λ, fitting the exponential ansatz to the data, and evaluating the fit at $\lambda = 0$.

The approach that is simplest and least prone to error is to only gather data for odd λ. However, each time λ is increased to the next odd integer, the circuit depth increases by $2d$. After only a few values of λ, the depth may be too large for a given quantum processor to handle without introducing significant errors. To build a circuit with arbitrary $\lambda \geq 1$, which would result in a better fit, one needs precise knowledge of

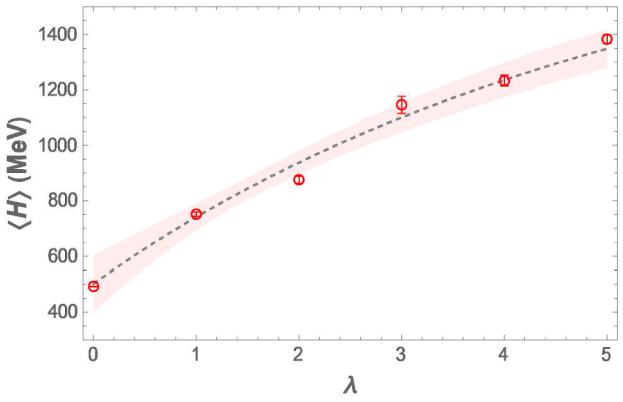

FIGURE 3. Expectation value (in MeV) of H_3, obtained by combining the plots in Fig. 2. Noiseless quantum simulation result is indicated by the star symbol for comparison.

each individual r_i. However, in this work we simply assume that each r_i is approximately equal, so that

$$\frac{\ln q}{\ln r} \approx \frac{s}{d} \tag{28}$$

and $\lambda \approx \kappa$. The result of applying this method to the 9 traceless unitaries in H_3 is illustrated in Fig. 2.

5. Measurements

We ran our circuit for calculating the 1S charmonium mass on IBMQ Athens. To calculate the expectation value of H_3 for a given α, β, λ, each of the 9 traceless unitaries in H_3 were measured separately 1.024×10^6 times. Beginning with $\lambda = 1$, we used the VQE algorithm to find the appropriate α and β. We then used this same approximate ground state wave function to calculate the expectation value of H_3 for $\lambda = 2, 3, 4, 5$. After applying the error mitigation technique discussed in the previous section, we measured $\langle H_3 \rangle (0)$ to be 502 ± 98 MeV, with the uncertainty given by 95% confidence mean prediction bands. This agrees well with the 493 ± 1 MeV we measured using the noiseless IBM QASM Simulator. Fig. 3 shows $\langle H_3 \rangle (\lambda)$ with total mean prediction bands and the zero-noise extrapolated result.

To measure the 2S expectation value of H_3, we orthogonalized the UCC ansatz with respect to our estimate of the ground state and applied the VQE algorithm once again. With this constraint, the variational principle provides an estimate of the first excited state. Using the noiseless QASM Simulator, this procedure gave a 2S energy of 1212 ± 2 MeV. We did not use a noisy quantum computer to calculate the 2S expectation value of H_3.

6. Conclusions

In this article, we demonstrated how heavy quark bound states can be simulated on a quantum computer using an effective potential and variational procedure. To compute the expectation value of the Hamiltonian with respect to the UCC ansatz, it was necessary to use the Jordan-Wigner transformation. Each part of the Hamiltonian could then be measured separately. By tuning the parameters of our ansatz using the VQE algorithm, we were able to estimate both the ground and first excited states of a spinless c-$\bar{c}$ pair on a noiseless quantum simulator. Using a zero-noise extrapolation method, we then measured the ground state on a noisy quantum computer and achieved agreement with the noiseless value. The goal of this research was to highlight the quantum computational method used to extract bound states from a spin-averaged potential model, not to reproduce the physical ground and first excited states of charmonium. The physical states may be obtained using the same method by using an appropriate spin-dependent potential.

1. I. C. Cloët et al., *Opportunities for Nuclear Physics & Quantum Information Science*, arXiv preprint (2019). https://arxiv.org/abs/1903.05453.
2. D. B. Zhang, H. Xing, H. Yan, E. Wang and S. L. Zhu, *Selected topics of quantum computing for nuclear physics*, Chinese Phys. B **30** (2021) 020306. https://doi.org/10.1088/1674-1056/abd761.
3. D. E. Kharzeev, *Quantum information approach to high energy interactions*, Phil. Trans. A. Math. Phys. Eng. Sci. **380** (2021) 20210063. https://royalsocietypublishing.org/doi/10.1098/rsta.2021.0063.
4. E. F. Dumitrescu *et al.*, *Cloud quantum computing of an atomic nucleus*, Phys. Rev. Lett. **120** (2018) 210501. https://doi.org/10.1103/PhysRevLett.120.210501.
5. H. H. Lu *et al.*, *Simulations of subatomic many-body physics on a quantum frequency processor*, Phys. Rev. A **100** (2019) 012320. https://link.aps.org/doi/10.1103/PhysRevA.100.012320.
6. N. Klco *et al.*, *Quantum-classical computation of Schwinger model dynamics using quantum computers*, Phys. Rev. A **98** (2018) 032331. https://link.aps.org/doi/10.1103/PhysRevA.98.032331.
7. N. Klco and M. J. Savage, *Digitization of scalar fields for quantum computing*, Phys. Rev. A **99** (2019) 052335. https://link.aps.org/doi/10.1103/PhysRevA.99.052335.
8. A. Roggero and J. Carlson, *Dynamic linear response quantum algorithm*, Phys. Rev. C **100** (2019) 034610. https://link.aps.org/doi/10.1103/PhysRevC.100.034610.
9. D. Lee *et al.*, *Projected Cooling Algorithm for Quantum Computation*, Phys. Lett. B **807** (2020) 135536.

https://link.aps.org/doi/10.1016/j.physletb.2020.135536.

10. H. Lamm, S. Lawrence and Y. Yamauchi, *General methods for digital quantum simulation of gauge theories*, Phys. Rev. D **100** (2019) 034518. https://link.aps.org/doi/10.1103/PhysRevD.100.034518.
11. A. Alexandru, P. F. Bedaque, S. Harmalkar, H. Lamm, S. Lawrence and N. C. Warrington, *Gluon field digitization for quantum computers*, Phys. Rev. D **100** (2019) 114501. https://link.aps.org/doi/10.1103/PhysRevD.100.114501.
12. A. Ciavarella, N. Klco and M. J. Savage, *Trailhead for quantum simulation of SU(3) Yang-Mills lattice gauge theory in the local multiplet basis*, Phys. Rev. D **103** (2021) 094501. https://link.aps.org/doi/10.1103/PhysRevD.103.094501.
13. Y. Y. Atas, J. Zhang, R. Lewis, A. Jahanpour, J. F. Haase and C. A. Muschik, *SU(2) hadrons on a quantum computer via a variational approach*, Nat. Commun. **12** (2021) 6499. https://doi.org/10.1038/s41467-021-26825-4.
14. T. D. Cohen, H. Lamm, S. Lawrence and Y. Yamauchi, *Quantum algorithms for transport coefficients in gauge theories*, Phys. Rev. D **104** (2021) 094514. https://doi.org/10.1103/PhysRevD.104.094514.
15. T. Li, X. Guo, W. K. Lai, X. Liu, E. Wang, H. Xing, D. B. Zhang and S. L. Zhu, *Partonic Structure by Quantum Computing*, arXiv preprint (2021). https://arxiv.org/abs/2106.03865.
16. D. E. Kharzeev and Y. Kikuchi, *Real-time chiral dynamics from a digital quantum simulation*, Phys. Rev. Res. **2** (2020) 023342. https://doi.org/10.1103/PhysRevResearch.2.023342.
17. Z. Tu, D. E. Kharzeev and T. Ullrich, *Einstein-Podolsky-Rosen Paradox and Quantum Entanglement at Subnucleonic Scales*, Phys. Rev. Lett. **124** (2020) 062001. https://doi.org/10.1103/PhysRevLett.124.062001.
18. J. R. McClean, J. Romero, R. Babbush and A. Aspuru-Guzik, *The theory of variational hybrid quantum-classical algorithms*, New J. Phys. **18** (2016) 023023. https://doi.org/10.1088/1367-2630/18/2/023023.
19. Y. Shen, X. Zhang, S. Zhang, J. Zhang, M. Yung and K. Kim, *Quantum implementation of the unitary coupled cluster for simulating molecular electronic structure*, Phys. Rev. A **95** (2017) 020501. https://doi.org/10.1103/PhysRevA.95.020501.
20. D. Gallimore and J. Liao, *Quantum Computing for Heavy Quarkonium Spectroscopy*, arXiv preprint (2022). https://arxiv.org/abs/2202.03333.
21. H. S. Chung, J. Lee and D. Kang, *Cornell Potential Parameters for S-Wave Heavy Quarkonia*, J. Korean Phys. Soc. **52** (2008) 1151. https://doi.org/10.3938/jkps.52.1151.
22. E. A. Hylleraas and B. Undheim, *Numerische Berechnung der 2S-Terme von Ortho- und Par-Helium*, Zeitschrift für Physik **65** (1930) 759. https://doi.org/10.1007/BF01397263.
23. J. K. L. MacDonald, *Successive Approximations by the Rayleigh-Ritz Variation Method*, Phys. Rev. **43** (1933) 830. https://link.aps.org/doi/10.1103/PhysRev.43.830.
24. M. A. Nielsen and I. L. Chuang, Quantum Computation and Quantum Information, 10th Anniversary ed. (Cambridge University Press, Cambridge, UK, 2011), pp. 373–385.
25. T. Giurgica-Tiron, Y. Hindy, R. LaRose, A. Mari and W. J. Zeng, Digital zero noise extrapolation for quantum error mitigation, 2020 IEEE International Conference on Quantum Computing and Engineering (2020) 306–316. https://doi.org/10.1109/QCE49297.2020.00045.